



## Research article

## Adsorption of anionic dyes from textile wastewater utilizing raw corncob

Shameran Jamal Salih<sup>a,\*</sup>, Aram Salahuddin Abdul Kareem<sup>b</sup>, Sewgil Saaduldeen Anwer<sup>c,d</sup><sup>a</sup> Department of Chemistry, Faculty of Science and Health, Koya University, Koya KOY45, Kurdistan Region - F.R. Iraq<sup>b</sup> Department Medical Lab. Science, Lebanese French University, Kurdistan Region, Iraq<sup>c</sup> Clinical Biochemistry Department, College of Health Sciences, Hawler Medical University, Kurdistan Region, Iraq<sup>d</sup> Nursing Department, Nursing Faculty, Tishk International University, Kurdistan Region, Iraq

## ARTICLE INFO

## Keywords:

Dye removal

Adsorption

Corncob waste

Wastewater treatment

## ABSTRACT

Toxic dyes are irrefutable effluent components of textile wastewater, so they have become a major economic and health concern. With the purpose of efficient removal of textile dyes, multiple nature-inspired adsorbents have been applied. Herein, raw corncob is proposed as a novel highly efficient, low-price, and abundantly attainable adsorbent with the potential for uptake of methyl red and methyl orange. Multiple experiments were carried out to optimize parameters including pH, primary concentration, adsorbent dosage, temperature, and contact time. The adsorption was raised with the mounting of the contact time and it was alleviated with the addition of initial concentration. The foremost uptake of dye was apperceived at an acidic medium pH 4 for methyl red and pH 1 for methyl orange. Scanning Electron Microscopy and Fourier Transform Infrared Spectroscopy were employed to characterize the surfaces of corncobs. The well-fitted Langmuir and Freundlich models (methyl red:  $R^2 = 0.9956$  and methyl orange:  $R^2 = 0.9883$ ) confirmed the homogeneous monolayer adsorption process on the raw corncob surface. The obtained results disclose that corncob is an effectual biosorbent for eliminating anionic dyes without the necessity for any prior modifications.

## 1. Introduction

Textile industries positively influence economic development, worldwide. However, one of the obstacles associated with textile manufactories is undesirable dye effluent. The textile industry has a high position in the use of dyes among other industries for the dyeing of fibers [1]. It also releases a maximum amount of dye effluents into the environment [2]. It is estimated that nearly 280,000 tons of dyestuff, which is 10%–15% of total dyes applied during the synthesis of textile products, are discharged every year [3].

Textiles are composed of both natural and synthetic fibers. They are used as raw feeds to prepare many kinds of garments. One ton of natural and synthetic textiles need almost 60 m<sup>3</sup> and 92 m<sup>3</sup> of fresh water, respectively, and result in 17%–20% of discharges into wastewater. These volumes of effluents are produced in each of the processes such as dyeing, scouring, printing, sizing, mercerizing, de-scouring, bleaching, and finishing [4]. The incapability of dye mixture adsorption onto the fabric results in the discharge of dye effluents. Fabrics can only absorb 25% of the dye mixture because of their limited absorption potential [5].

Dye is a colored substance and absorbs a certain wavelength in the visible spectrum range. It has a relatively stable and complicated

aromatic structure that is also resistant to degradation [6]. Dyes are mostly utilized in the pharmaceutical, textile, cosmetics, food, plastics, photographic, and paper industries [7]. According to the resources, dyes are mainly categorized into synthetic and natural ones. Natural dyes are based on plants or animals. On the other hand, the synthetic dyes are grouped into azo and non-azo dyes. Azo dyes are further categorized into the acidic, reactive, basic, vat, disperse, and sulfur dyes [8]. Methyl orange (MO) and methyl red (MR) are two examples of acidic dyes that are used as dyes.

Recently, several reports have been published regarding dye removal methods [9, 10, 11, 12, 13]. These methods are capable of removing dyes in a small timescale. The presented methods could be classified into three significant treatment categories including chemical, biological, and physical treatments. Advanced oxidation (AOP), electrochemical treatment, adsorption, biological treatment, and membrane filtration are some of the remarkable techniques which are generally utilized for dye elimination [14, 15, 16, 17, 18]. Each method has some benefits and disadvantages. Adsorption is the most commonly utilized method. It allows for removing low to high pollutants concentrations. Therefore, many studies have been performed to develop effective and price-effective adsorbent materials.

\* Corresponding author.

E-mail addresses: [shameran.jamal@koyauniversity.org](mailto:shameran.jamal@koyauniversity.org), [shameran.salih.cy@gmail.com](mailto:shameran.salih.cy@gmail.com) (S.J. Salih).

The agricultural wastes are used to remove contaminations in the wastewater due to their easy availability. Moreover, they have favorable physicochemical traits like high adsorption capacity and good removal efficiency. They are also renewable with or without prior processing like grinding, washing, and drying. In this way, they decrease the additional energy costs as well as production costs in the case of thermal treatments [19]. Agricultural wastes are mostly containing hemicellulose, lignin, and cellulose of high molecular weight. Some small-sized lignocellulosic materials are much important for the removal of dye molecules [20, 21, 22]. The agricultural wastes have been successfully applied for basic excluding of dyes as well as acid dyes. The maximum adsorption of cationic dyes occurs in the pH ranging from 6–10, while removal of acid dyes is favored at pH 2–4. At the acidic pH range, the positively charged adsorbent surface is proper to adsorb negatively charged anionic dyes. On the other hand, the surface of the adsorbent attains negative charges at the basic pH range thus appropriate for the uptaking of the positively charged cationic dye. The agricultural wastes show a maximum potential for cationic dyes followed by anionic dyes [23, 24].

Corn cob is abundant, develops wide surface areas, and is cost-effective. These traits make the corn cob an appropriate adsorbent for the treatment of textile effluents. Furthermore, due to the presence of charges on the surface, porosity, and layered structures, the corn cob has been proposed as an efficient adsorbent for the excluding of organic or inorganic contaminants from wastewater [25, 26].

To the best of our knowledge, there are very few reports regarding the importance of the removal of dye wastewater utilizing raw corn cob [27, 28]. Therefore, for the first, the possibility of employing raw corn cob to remove MR and MO from textile wastewater was surveyed. The outcomes

reveal the adsorbent potential of corn cob powder for dye elimination from wastewater.

## 2. Materials and methods

### 2.1. Materials

Corn cob was prepared from a local market that had collected as agricultural wastes from agricultural fields. It was leached with double distilled water to eliminate dust contaminations. Afterward, it was dried in open air followed by controlled drying at 70 °C in an oven for 24 h. The dried corncobs were crushed into small pieces with the help of a corn cob crusher machine followed by grinding in a maize grinding machine to produce powder form. The resulting corn cob media was then sieved by passing it through a set of ASTM standard sieves with mesh sizes of 60–200 to generate fractions with various particle sizes in the range of 250–74 μm. Finally, 0.075 mm size particles of corn cob were selected as an adsorption media. The sieved fractions were kept in airtight plastic stacks for future use. MR and MO were purchased from Sigma-Aldrich. The stock solutions of dyes were supplied by appending 1 g of each dye powder to 1000 ml of double-distilled water.

### 2.2. Adsorption experiments

The adsorption tests were performed by adding 1g of adsorbent to a volume of 100 ml dye in a conical flask with a volume of 250 ml. The primary pH of the dye solution was set by appending 0.1M NaOH or 0.1M HCl. Corncobs were then appended to the dye solution and were shaken

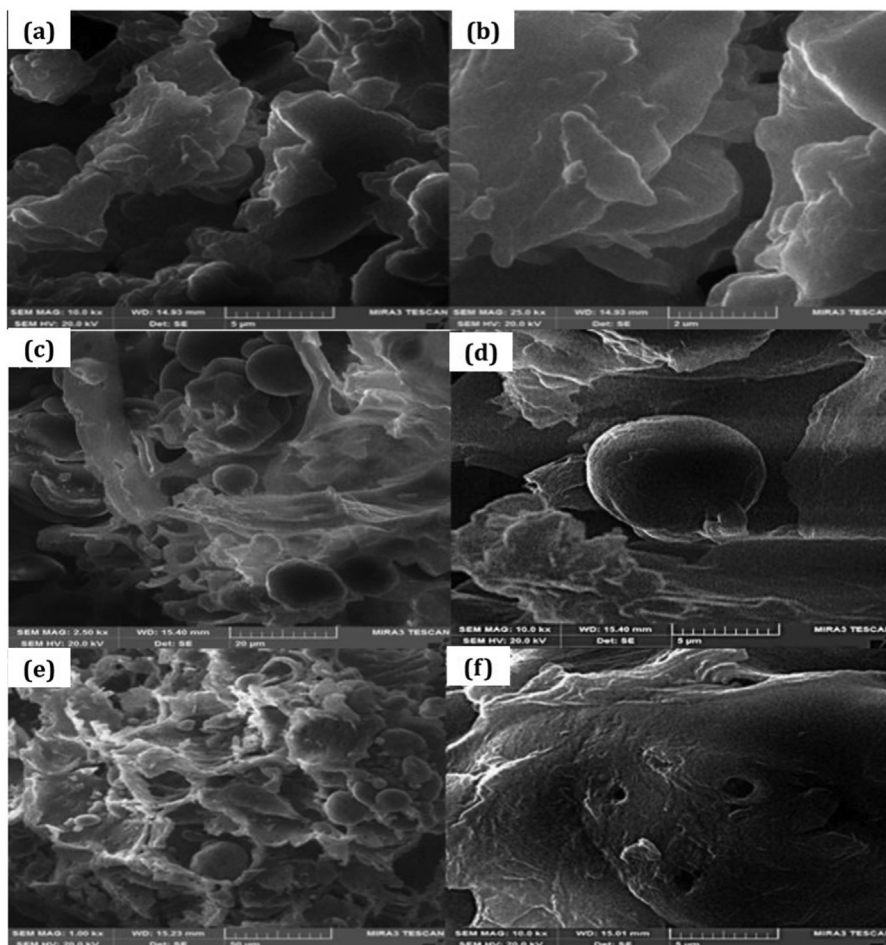


**Figure 1.** (a) SEM analysis of raw corn cob before adsorption of dyes. (b) The magnified encircled part of the corn cob. (c) SEM analysis of raw corn cob after MR adsorption. (d) The magnified encircled part of the corn cob. (e) SEM analysis of raw corn cob after MO adsorption. (f) The magnified encircled part of the corn cob.

at the temperature of 30 °C until the equilibrium was obtained. After the adsorption process, the samples were gathered, and the suspensions were detached using filter paper. The conical flask was placed in the rotary shaker with stirring of 180 rpm at room temperature. After filtration, the dye elimination was surveyed.

The amount of adsorption capacity (amount of dyes per unit mass) and the removal efficiency were determined using the equations [1] and [2], respectively:

$$q_e = \frac{C_o - C_e}{W} \times V \quad (1)$$

$$R\% = \frac{C_o - C_e}{C_o} \times 100 \quad (2)$$

Where,

- $q_e$  = Amount of adsorbed dyes (mg/g)
- $C_o$  = Primary concentration (mg/l)
- $C_e$  = Equilibrium concentration (mg/l)
- $W$  = Mass of adsorbent (mg)
- $V$  = Solution volume (ml)
- $R\%$  = Removal percentage

Moreover, Langmuir and Freundlich isotherm models were applied to analyze the data. The liner forms of Langmuir and Freundlich models are represented in equations [3] and [4], respectively:

$$\frac{C_e}{q_e} = \frac{1}{q_m K_L} + \frac{C_e}{q_m} \quad (3)$$

$$\log(q_e) = \log K_f + \frac{1}{n} \log C \quad (4)$$

Where,  $C_e$  is the concentration of dyes at equilibrium in (mg/l),  $q_e$  is the value of dyes adsorbed per unit mass,  $K_L$  is the Langmuir constant,  $q_m$  is the uppermost adsorption capacity in (mg/g),  $K_f$  and  $n$  are Freundlich constants which determine the favorability of the adsorption process.

### 2.3. Instruments

Fourier transform infrared spectroscopy (FT-IR) was carried out by Bio-Rad Merlin, FT-IR spectroscopy Mod FTS 3000. Surface morphology analysis was performed by scanning electron microscopy (SEM, NORAN at an electron acceleration voltage of 25kV). UV-Visible spectroscopy measurement was accomplished using a double beam spectrophotometer NORAN at  $\lambda_{max}$  464nm (methyl Orange) and  $\lambda_{max}$  410nm (methyl red).

## 3. Results and discussion

### 3.1. Morphology characterization

SEM images of corncobs powder were surveyed to analyze the morphological surface before and after adsorption of dyes on the adsorbent surface. Figure 1a indicates the SEM image of the coarsened surface of corncobs before the adsorption of dyes. The encircled part is magnified in Figure 1b. The cracks are observed in the encircled portion. The coarse surface and the cracks facilitate the adsorption phenomenon. Figure 1c and Figure 1e show the SEM images of MR-loaded and MO-loaded corncob surfaces, respectively. The magnified encircled parts clearly indicate the binding of dye particles on the adsorbent surface (Figure 1d and Figure 1f, respectively) [29].

### 3.2. FT-IR analysis

The functional groups present on the corncob surface were determined by FT-IR analysis. FT-IR spectra of corncob before and after

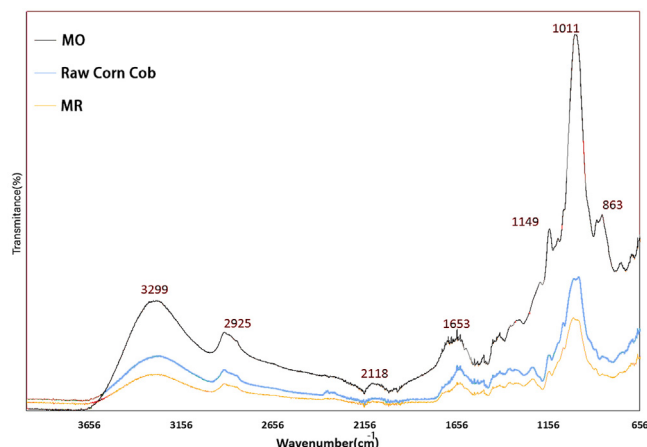


Figure 2. FTIR analysis of raw corncob and MO- and MR-loaded corncob.

adsorption of MO and MR are indicated in Figure 2. The peaks at 3299  $\text{cm}^{-1}$  show the O–H stretching due to the presence of hydrogen bonding or alcoholic bonding. They also denote the presence of water molecules in the corncob adsorbent. A little peak at 2925  $\text{cm}^{-1}$  reveals the C–H stretching which is ascribed to the bonding present in the organic adsorbents [30]. Another peak at 1653  $\text{cm}^{-1}$  is ascribed to C=N and C=C stretching [31]. The C–N and C–H bonding appearing at 1149  $\text{cm}^{-1}$  and 1202  $\text{cm}^{-1}$ , respectively, show the attendance of aromatic amines,  $\text{CH}_2$ , and  $\text{CH}_3$ . The most prominent peak of MO at 1011  $\text{cm}^{-1}$  shows the aliphatic amines. The same but smaller peak is observed for MR and raw corncob. Another differentiate peak at 806  $\text{cm}^{-1}$  shows the attendance of C–H stretching of aromatics after adsorption [32].

### 3.3. Effect of adsorbent dose

The dose efficacy of the adsorbent was surveyed ranging from 0.05 to 5  $\text{g.L}^{-1}$  of an adsorbent. Figure 3 shows the removal efficiency at various adsorption doses (corncob = 20  $\text{mg.L}^{-1}$ , contact time = 100 min, and temperature = 25 °C). The removal percentages were considerably increased from 8.8 to 94.54% for MR (Figure 3a) and from 15.23 to 99.25% for MO (Figure 3b), with the quantized increment of adsorbent dose from 0.05 to 5.0  $\text{g.L}^{-1}$ . The enhancement in the removal percentage with the elevation of the adsorbent dose is owing to the increase of the adsorbent surface area and consequently accessibility to more binding sites [33]. Besides, the reverse trend in the adsorption capacity of the adsorbent was seen. The capacity of adsorption decreased significantly from 3.53 to 0.378  $\text{mg/g}$  for MR and from 6.09 to 0.397  $\text{mg/g}$  for MO with the enhancement in the corncob dose from 0.05 to 5.0  $\text{g/L}$ . The decline in the adsorption capacity along with an elevation in the corncob dose is due to the bump or cluster of adsorbent particles that are formed because of cohesive interactions. It results in the reduction of effective surface area per unit weight (g) of adsorbent. Moreover, data did not indicate any significant MR removal (0.85–0.378  $\text{mg.g}^{-1}$ ) and MO removal (0.88–0.39  $\text{mg.g}^{-1}$ ) at corncob dose from 2.0 to 5.0  $\text{g.L}^{-1}$ . It could be ascribed to the overcrowding of adsorbent biomass resulting in the overlapping of sorption sites [34]. In other words, some active binding sites remain unsaturated during the sorption process [35]. Therefore, both negative and positive effects of elevating adsorbent doses were considered for further studies.

### 3.4. Effects of temperature

The temperature effect on the adsorption of dye is indicated in Figure 4. Outcomes illustrate that appending temperature from 25 to 40 °C decreases the adsorption of dye which confirms the exothermic nature of this process. The decrease in percentage removal for MR and MO with increasing temperature can be attributed to several reasons: i) increasing

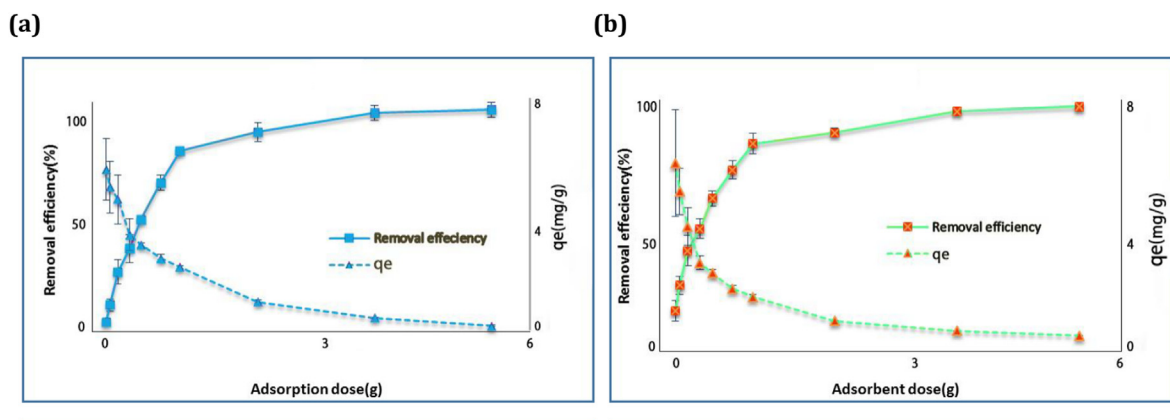


Figure 3. Effect of adsorbent dose on (a) MR and (b) MO adsorption.

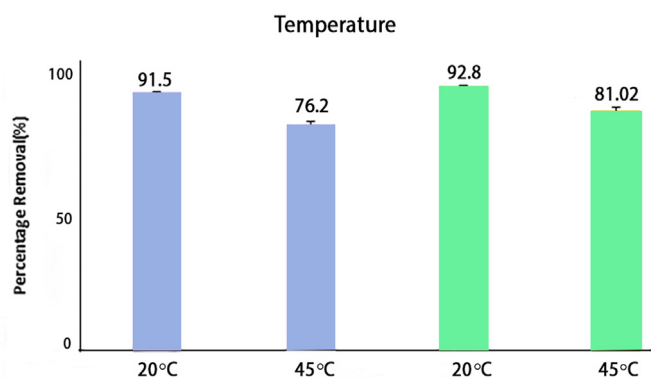


Figure 4. Effect of temperature on MR (red color) and MO (orange color) adsorption.

the solubility of MR and MO in water; ii) the stronger interaction of dye-solvent than the dye-adsorbent interaction; iii) higher Brownian movement of MR and MO molecules in the solution; iv) the dissociation of hydrogen bonding between dyes and corncob, v) damaging the active sites on the surface of adsorbent [36]. The graph demonstrates the negative effect of temperature on the corncob adsorption capacity for anionic acidic dyes. It affects the chemical potential of the adsorbent since the system mobility increases but the interactions decrease [37].

### 3.5. Effect of pH

The solution pH is the foremost crucial factor in the adsorption. It can alter the adsorbent surface charge. It can also affect the adsorption kinetics by changing the solubility of dyes or ionization state. Figure 5a-b show the adsorption of dyes on the corncob surface at various pHs [1, 2, 3, 4, 5, 6, 7, 8, 9, 10, 11]. It has been observed that corncob has the

potential to adsorb MR and MO from an aqueous solution at different pH levels. The highest levels of removal efficiency of MR and MO occurred at pH 4 and 1, respectively. This indicates that the adsorbent is selective for the anionic dyes at only acidic pH. The pH<sub>pzc</sub> of corncob was 6.83 and 6.2, therefore, the corncob particles have positive charges in pH below these values [38, 39]. The positive charge of the corncob surface at acidic pH is owing to the protonated binding sites. The protonation helps the anionic dye adsorption owing to the electrostatic attraction. Consequently, lower pH causes the premiere protonation of the corncob surface leading to the better adsorption of dyes. There is a remarkable electrostatic attraction between anionic MO and the positively charged surface of the adsorbent at low pH (4 and below). With the addition of pH, the negatively charged sites increase. Therefore, the adsorption of anions is decreased because of the negatively charged sites on the surface of the adsorbent leading to electrostatic repulsion. It is found that adsorption was somewhat unfavorable at pH lower than 4 for MR [32]. This is ascribed to the addition of the proton concentration which in turn results in the constitution of aqua complexes and holds back the dye sorption [40]. Moreover, at alkaline pH, lower adsorption of both dyes is attributed to excess OH ions, thus competing for the adsorption in the active sites of the adsorbent [41]. In acidic media, the adsorption of MR and MO on the corncob surface is relatively physisorption, not chemisorption [39]. Different types of forces like weak Van der Waals forces and relatively stronger electrostatic attractions exist between the ionized form of sulfonyl substitutions on the dye molecules and the positively charged surface of the corncob (Eqs. (5) and (6)).

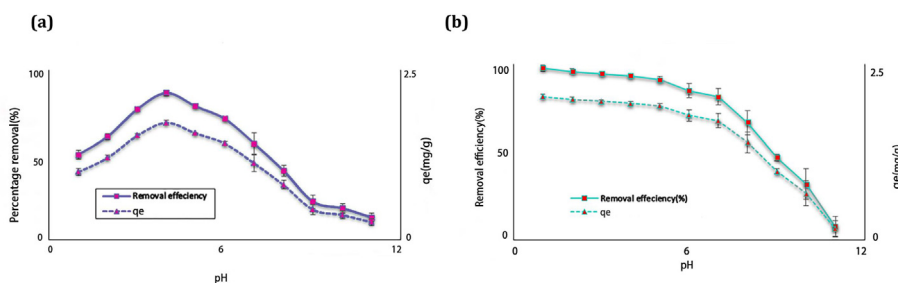
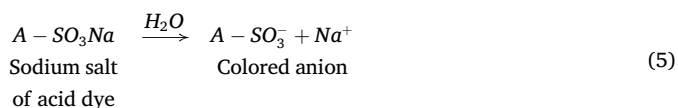
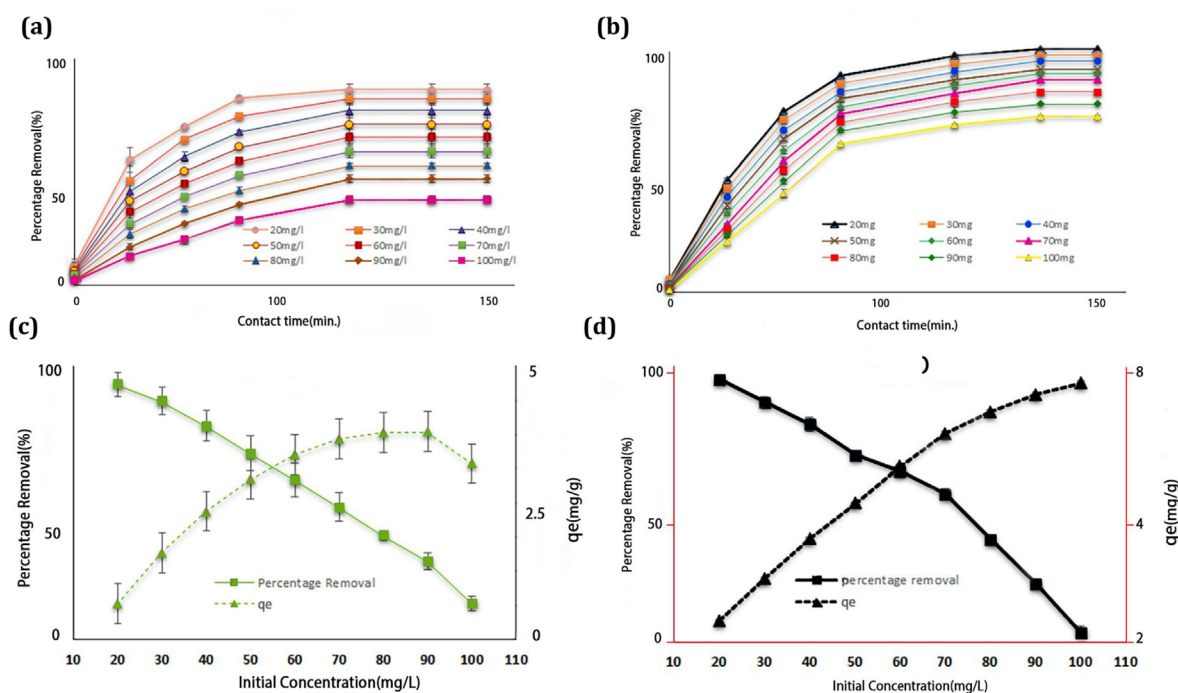


Figure 5. Effect of pH on adsorption of (a) MR and (b) MO.



**Figure 6.** Effect of contact time on adsorption of (a) MR and (b) MO; Effect of initial concentration of (c) MR and (d) MO on the adsorption process.

### 3.6. Effect of initial dye concentration and contact time

The efficacy of primary dye concentration and contact time were surveyed utilizing various concentrations MR and MO solutions (20, 30, 40, 50, 60, 70, 80, 90, 100 mg/L) and then agitation with 1g of corncob at 25 °C for 0, 20, 40, 60, 100, 130, and 150 minutes as shown in Figure 6a-d. It has been found that removal efficiency enhances with increasing contact time and decreases with the rise of primary concentration. From the current study, it is obvious that contact time has a prominent effect on adsorption. Adsorption efficiency steadily increases with contact time for all initial concentration values [43]. Additionally, regardless of initial concentration, the adsorption rate was initially rapid as the maximum number of positively charged binding sites was present for adsorption. The driving force was initially strong for the dye adsorption on the surface of adsorbent. However, the driving force and unsaturated sites were decreased. It resulted in a slower adsorption rate. Then, dynamic equilibrium was attained [41, 44]. Figures 6a-b show that in the different concentrations of dyes, the adsorption rate was higher initially which decreased slowly till the equilibrium point was reached. The required contact time for MR solution to reach equilibrium was found to be 100 minutes while for MO solution was 130 minutes. Therefore, the experiments were continued for 150 minutes. At low concentrations, the ratio of the primary amount of dyes to the accessible vacant sites of adsorbent is small. So, the fractional adsorption is not dependent on the initial adsorbate concentration. There are dual challenges for the dye molecules in the process of adsorption including the counteraction of the boundary layer efficacy and the adsorption on the surface of adsorbent [42, 45].

The effect of primary dye concentration on the capacity of adsorption and removal efficiency is shown in Figures 6c-d. In the case of MR adsorption, the adsorption capacity improves gradually from 1.72 to 4.24 mg/g for the primary concentrations of 20–90 mg/L. The dye uptake then decreased for dye concentrations higher than 90 mg/L because of the saturation of sorption sites on the surface of adsorbent [46]. The increase of adsorbed dye at equilibrium from 1.96 to 7.10 mg/g was associated with an increment in the primary concentration of MO dye from 20 to 100 mg/L. The primary concentration of dye supplies the driving force to dominate the resistance between the solid and aqueous phases. Therefore, the mass transfer of dyes occurs from the aqueous to the solid phase.

With the growth in the primary concentration of dye, the interaction between the adsorbate and adsorbent increases. The same behavior is also observed in the adsorption of the MO at the surface of mesoporous carbon [47, 48]. If the adsorbent dose is kept constant, the binding sites become saturated and cannot further accommodate the higher concentration of adsorbate. So, the initial concentration limits the removal percentage [49]. Conversely, the increase in  $C_0$  accelerates the interaction between the adsorbent and dye. Therefore, a higher adsorption capacity is achieved at high  $C_0$  [50].

### 3.7. Langmuir isotherm

The isotherm models for modeling the experimental data are demonstrated in Figure 7. The different constants of Langmuir are listed in Table 1. In the current study, the Langmuir model is the best-fitted isotherm model with the maximum correlation coefficient values as  $R^2 = 0.9956$  and  $R^2 = 0.9883$  for MO and MR, respectively, which reveal the monolayer adsorption on a homogeneous adsorbent surface. This is a common traditional model used for the calculation of  $q_{max}$  when an adsorbent surface becomes saturated [43]. There is a uniform distribution of energy all over the adsorbent surface with finite active sites and fixes the position of adsorbate molecules with no movement.

A plot of  $q_e$  versus  $q_e/C_e$  at various initial concentrations (20–100 mg L<sup>-1</sup>) shows the slope and intercept (Figure 7a-b). The correlation coefficients  $R^2 = 0.9956$  and  $R^2 = 0.9883$  and maximum monolayer capacity (7.50 mg/g and 4.29 mg/g) for MO and MR, respectively, provide big evidence of the Langmuir fit. The key characteristic of the Langmuir isotherm model is a dimensionless constant  $R_L$  which is equal to 0.1 for MO and 0.09 for MR. These values confirm the efficacy of corncob as an appropriate adsorbent for both dye removals at optimized conditions. However, a greater value of  $R^2$  for MO reveals that the adsorption of corncob on MO is higher than MR [51].

### 3.8. Freundlich isotherm

Freundlich isotherm shows multilayer adsorption on the heterogeneous surface of an adsorbent as shown in Figure 8. The different constants of Freundlich are listed in Table 2. Both amounts of  $K_f$  and  $1/n$  are

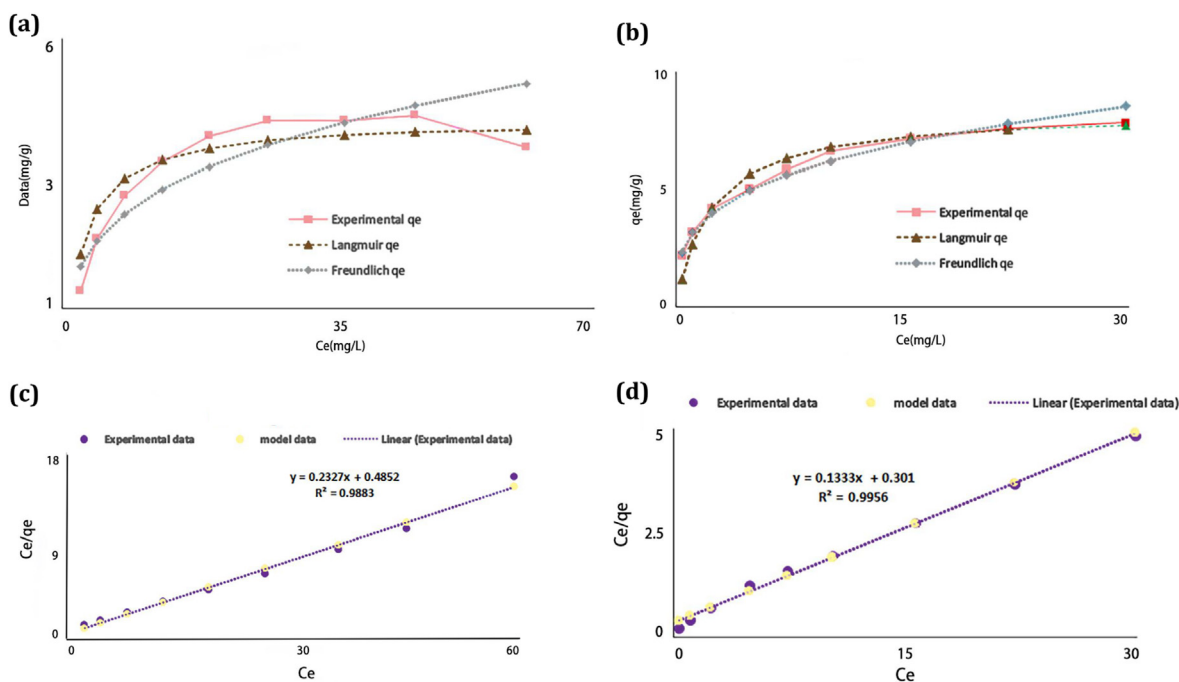


Figure 7. Experimental data and fitted plots of Langmuir and Freundlich models for the adsorption of (a) MR and (b) MO; Langmuir isotherm model of (c) MR and (d) MO.

Table 1. Different constants of Langmuir isotherm models.

Dyes	Parameters	Units	Values
Methyl Orange	$q_{exp}$	$(mg.g^{-1})$	6.966591
	$q_{max}$	$(mg.g^{-1})$	7.501875
	$K_L$	$(L.mg^{-1})$	0.442857
	$R^2$		0.9956
Methyl Red	$q_{exp}$	$(mg.g^{-1})$	4.155489
	$q_{max}$	$(mg.g^{-1})$	4.297379
	$K_L$	$(L.mg^{-1})$	0.479596
	$R^2$		0.9883

Table 2. Different constants of Freundlich isotherm models.

Dyes	Parameters ( $L.mg^{-1}$ )	Values
Methyl Orange	$K_f$	2.801906
	$1/n$	0.2993
	$n$	3.341129
	$R^2$	0.9864
Methyl Red	$K_f$	1.68725
	$1/n$	0.2562
	$n$	3.903201
	$R^2$	0.831

obtained from the plot of  $\ln q_e$  versus  $\ln C_e$ , which are  $1.68 L.mg^{-1}$  and  $0.256$  for MR (Figure 8a) and  $2.80 L.mg^{-1}$  and  $0.299$  for MO, respectively (Figure 8b).  $K_f$  and  $1/n$  values show the strength and functionality of the adsorption. Freundlich exponent ( $1/n$ ) must be between 0 and 1 for desirable adsorption. The value of  $1/n$  quantifies the desirability of adsorption and the heterogeneity degree on the corncob surface. This confirmed the efficacy of raw corncob for dyes adsorption from the aqueous solution. The coefficient of determination values was  $R^2 =$

$0.9864$  for MO and  $0.831$  for MR indicating that the model is fitted with experimental data but less fit than the Langmuir model. Moreover, it shows the supremacy of active sites with homogeneous energy distribution. The value of  $n = 3.34$  for MO and  $3.90$  for MR represent that adsorption on corncob is a favorable process for both dyes as the amount of  $n$  must be between 1 and 10 for favorable adsorption [52]. The higher values of  $R^2$  for the Langmuir model of both dyes confirm the suitability of the model for dye adsorption on corncob followed by the Freundlich

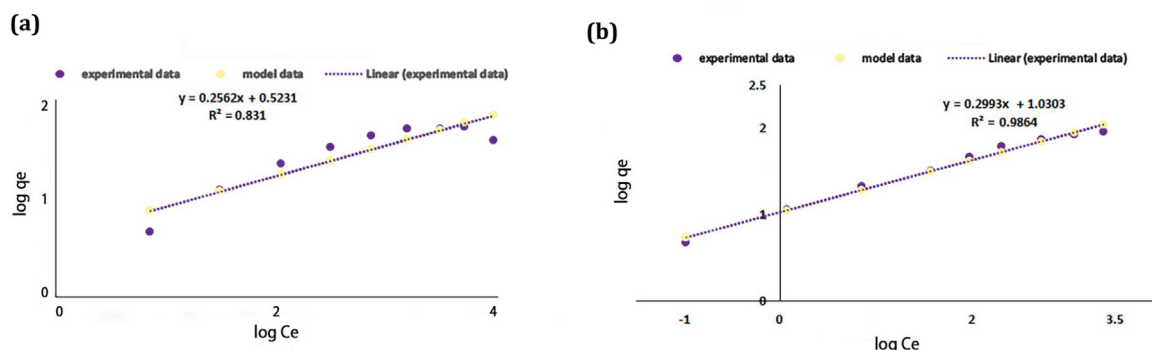


Figure 8. Freundlich isotherm model of (a) MO and (b) MR.

**Table 3.** Recently published papers reporting in the dye removal from wastewater.

Adsorbent	Dyes	PH range	Removal %	Adsorption Capacity (q <sub>e</sub> ) (mg/g)	References
Lemongrass leaf	MR	2	63.87%	15.97 mg/g	[56]
Sugarcane press mud	MO	2	98.68%	2.5978 mg/g	[57]
Eggshell	MO	-	27.70%	25 mg/g	[58]
White potato peel	MR	2	86.58%	5.62 mg/g	[59]
Coconut shell	MO	2	50.707%	0.247 mg/g	[60]
Mahagoni (Swietenia mahagoni) Bark	MO	3	92%	6.071 mg/g	[61]
Mandarin Peel	MO	7	97%	2.52 mg/g	[62]
Orange peel	MR	1	33.33%	3.97 mg/g	[63]
(Present Work) Corncob	MR and MO	4	94.54%	3.53 mg/g	-
		1	99.54%	6.09 mg/g	

model. This indicates the relevancy of both isotherm models for MR and MO adsorption on raw corn cob adsorbent [53].

The values of isotherm models indicate that experimental data is well fitted with Langmuir data than Freundlich data for both dyes. It is therefore deduced that the adsorption of both dyes on the surface of raw corncob is homogeneous in nature [54].

### 3.9. Estimating the effectiveness of raw corncob powder for real textile wastewater treatment

Considering the bulk availability of corncob residues in MT/year in Iraq, the process can be recommended for real wastewater containing MR or MO. The availability of corncobs can be calculated as Eq. (7):

$$R_{\text{cob}} = \text{Grain yield} * \text{CGR} * \text{Removal \%} * [1 - \text{Moisture\%}] \quad (7)$$

Where  $R_{\text{cob}}$  is called the quantity of dried harvestable cobs (tones/acre), grain yield is the average yield of grain crop (tones/acre) which is equal to 3.5 metric tons/hectare or 1.42 tones/hect. The cob-to-grain ratio or CGR is 1:5.6. The percent of removal is the percent of removed cobs from fields every year which is equal to 1. The moisture content of corncob is equal to 20%. So,  $R_{\text{cob}}$  is obtained as 0.2 ton/acre of corncob [55]. The total area in Iraq under maize cultivation is 0.9 million hectares, thus, the total maize cob production in Iraq can be obtained by Eq. (8):

$$\begin{aligned} \text{Total maize cob production in Iraq} &= R_{\text{cob}} * \text{Total area under cultivation} \\ &= (0.2 \text{ tones/acre}) * (0.9 \text{ million Hectare}) \\ &= (0.2 \text{ tones/acre}) * (0.222 * 10^5 \text{ acre}) \\ &= 4.44 * 10^5 \text{ tones} = 4 * 10^{11} \text{ grams} \end{aligned} \quad (8)$$

Now, by considering  $q_e = 7.67 \text{ mg/g}$  and primary concentration of dye = 20 mg/L, the adsorbent usage rate and treated textile wastewater can be obtained by Eqs. (9) and (10), respectively, as follow:

$$\text{Adsorbent usage rate} = C_o / q_t = (20 \text{ mg / L}) / (7.67 \text{ mg / g}) = 2.6 \text{ g / L} \quad (9)$$

$$\begin{aligned} \text{Textile wastewater to be treated} \\ &= \text{total maize cob production} / \text{adsorbent usage rate} = 4 * 10^{11} / 2.6 \\ &= 1538 \text{ million.m}^3 \end{aligned} \quad (10)$$

So with this rough estimation, approximately 1538 million.m<sup>3</sup> capacity of anionic dyes in wastewater can be treated using maize cobs as adsorbents.

Table 3 shows the results of using other adsorbents for removing MO and MR. The efficiency of the adsorbent used in this study is higher than theirs.

## 4. Conclusions

This study proposes the cost-efficient elimination of anionic dyes as the major effluent of textile industries. The higher adsorption capacity was obtained as 3.53 and 6.09 mg/g for MR and MO, respectively. The significant adsorption occurred in the first 100 min with 2.0 g.L<sup>-1</sup> of the corncob. The abundantly accessible corncob without needing any prior modification and treatment of wastewater are the major advantages of this process. The corncob residues showed a better function as adsorbents for MO rather than MR. During the adsorption of both MR and MO, the adsorption capacity decreases with the increase in temperature and pH. In the current research, the type of adsorption was found as Physisorption. Experimental data were well fitted with Langmuir data than Freundlich data for both dyes. It was therefore deduced that the adsorption of MR and MO on the raw corncob surface is homogeneous in nature. In addition, it was concluded that the utilization of corncob as an

adsorbent leads to a decrease in the inappropriate disposal of dyes into the environment.

## Declarations

### Author contribution statement

Shameran Jamal Salih: Conceived and designed the experiment; Performed the experiments; Analyzed and interpreted the data; Contributed reagents, materials, analysis tools or data; Wrote the paper.

Aram Salahuddin Abdul Kareem, Sewgil Saaduldeen Anwer: Analyzed and interpreted the data.

### Funding statement

This research did not receive any specific grant from funding agencies in the public, commercial, or not-for-profit sectors.

### Data availability statement

Data included in article/supplementary material/referenced in article.

### Declaration of interests statement

The authors declare no conflict of interest.

### Additional information

No additional information is available for this paper.

### References

- P. Kumar, A.J.S. Kumar, QiE. Research, In silico enhancement of azo dye adsorption affinity for cellulose fibre through mechanistic interpretation under guidance of QSPR models using Monte Carlo method with index of ideality correlation, SAR and QSAR Environ. Res. 31 (9) (2020) 697–715.
- R.G. Saratale, J.R. Banu, H.-S. Shin, R.N. Bharagava, G.D. Saratale, Textile Industry Wastewaters as Major Sources of Environmental Contamination: Bioremediation Approaches for its Degradation and Detoxification. Bioremediation of Industrial Waste for Environmental Safety, Springer, 2020, pp. 135–167.
- M. Baysal, K. Bilge, B. Yilmaz, M. Papila, Yürüm YJJoece, Preparation of high surface area activated carbon from waste-biomass of sunflower piths: kinetics and equilibrium studies on the dye removal, J. Environ. Chem. Eng. 6 (2) (2018) 1702–1713.
- D. Yaseen, M. Scholz, Textile dye wastewater characteristics and constituents of synthetic effluents: a critical review, Int. J. Environ. Sci. Technol. 16 (2) (2019) 1193–1226.
- J.Y. Chin, L.M. Chng, S.S. Leong, S.P. Yeap, N.H.M. Yasin, P.Y. Toh, et al., Removal of synthetic dye by *Chlorella vulgaris* microalgae as natural adsorbent, Arabian J. Sci. Eng. 45 (2020) 7385–7395.
- N. Ertugay, F.N. Acar, Removal of COD and color from Direct Blue 71 azo dye wastewater by Fenton's oxidation, Kinetic Study 10 (2017) S1158–S1163.
- L. Yang, J. Chen, S. Qin, M. Zeng, Y. Jiang, L. Hu, et al., Growth and lipid accumulation by different nutrients in the microalga *Chlamydomonas reinhardtii*, Biotechnol. Biofuels 11 (1) (2018) 40.
- H.X. Che, S.P. Yeap, A.L. Ahmad, J.J.C.E.J. Lim, Layer-by-layer assembly of iron oxide magnetic nanoparticles decorated silica colloid for water remediation, Chem. Eng. J. 243 (2014) 68–78.
- E. Rápo, K. Posta, M. Suciú, R. Szép, S. Tonk, Adsorptive removal of remazol brilliant violet-5R dye from aqueous solutions using calcined eggshell as biosorbent, Acta Chim. Slov. 66 (3) (2019) 648–658.
- E. Rápo, L.E. Aradi, Szabó Á, K. Posta, R. Szép, S. Tonk, Adsorption of remazol brilliant violet-5R textile dye from aqueous solutions by using eggshell waste biosorbent, Sci. Rep. 10 (1) (2020) 1–12.
- M. Gören, H.B. Murathan, K. Nihan, A.M. Murathan, Removal of rhodamine B from aqueous solution by using pine cone activated with HNO<sub>3</sub>, J. Int. Environ. Appl. Sci. 16 (3) (2021) 123–132.
- A. Ofomaja, K. Mtshatsheni, E. Naidoo, Synthesis and optimization of reaction variables in the preparation of pinemagnetite composite for removal of methylene blue dye, S. Afr. J. Chem. Eng. 29 (1) (2019) 33–41.
- T.A. Ojo, A.T. Ojedokun, O.S. Bello, Functionalization of powdered walnut shell with orthophosphoric acid for Congo red dye removal, Part. Sci. Technol. 37 (1) (2019) 74–85.
- S.O. Ganiyu, E.D. Van Hullebusch, M. Cretin, G. Esposito, M.A. Oturan, Coupling of membrane filtration and advanced oxidation processes for removal of pharmaceutical residues: a critical review, Separ. Purif. Technol. 156 (2015) 891–914.
- S. Samsami, M. Mohamadizani, M.-H. Sarrafzadeh, E.R. Rene, M. Firoozbahr, Recent advances in the treatment of dye-containing wastewater from textile industries: overview and perspectives, Process Saf. Environ. Protect. 143 (2020) 138–163.
- I. Oller, S. Malato, J. Sánchez-Pérez, Combination of advanced oxidation processes and biological treatments for wastewater decontamination—a review, Sci. Total Environ. 409 (20) (2011) 4141–4166.
- X. Chen, Z. Shen, X. Zhu, Y. Fan, W. Wang, Advanced treatment of textile wastewater for reuse using electrochemical oxidation and membrane filtration, WaterSA 31 (1) (2005) 127–132.
- M.J. Uddin, R.E. Ampia, W. Lee, Adsorptive removal of dyes from wastewater using a metal-organic framework: a review, Chemosphere 284 (2021), 131314.
- M. Rafatullah, O. Sulaiman, R. Hashim, A.J.Johm Ahmad, Adsorption of methylene blue on low-cost adsorbents: a review, J. Hazard Mater. 177 (1–3) (2010) 70–80.
- M. Liu, Q. Chen, K. Lu, W. Huang, Z. Lü, C. Zhou, et al., High efficient removal of dyes from aqueous solution through nanofiltration using diethanolamine-modified polyamide thin-film composite membrane, Separ. Purif. Technol. 173 (2017) 135–143.
- F.S. Mustafa, M. Güran, M. Gazi, Effective removal of dyes from aqueous solutions using a novel antibacterial polymeric adsorbent, J. Polym. Res. 27 (8) (2020) 1–11.
- A.M. Aljeboree, A.N. Alshirifi, A.F. Alkaim, Highly efficient removal of textile dye “DIRECT YELLOW (DY12) dyes” from aqueous systems using coconut shell as a waste plants, Plant Archives 20 (1) (2020) 3029–3038.
- X. Zhang, J. Zhou, Y. Fan, J. Liu, Adsorption of dyes from water by *Prunella vulgaris* stem and subsequent fungal decolorization, Kor. J. Chem. Eng. 37 (9) (2020) 1445–1452.
- A. Mohammadi, A. Alinejad, B. Kamarehie, S. Javan, A. Ghaderpoury, M. Ahmadvpour, et al., Metal-organic framework UiO-66 for adsorption of methylene blue dye from aqueous solutions, Int. J. Environ. Sci. Technol. 14 (9) (2017) 1959–1968.
- S. Samsami, M. Mohamadizani, M.-H. Sarrafzadeh, E.R. Rene, M. Firoozbahr, Recent advances in the treatment of dye-containing wastewater from textile industries: overview and perspectives, Process Saf. Environ. Protect. 143 (2020) 138–163.
- N. Abidi, J. Duplay, A. Jada, E. Errais, M. Ghazi, K. Semhi, et al., Removal of anionic dye from textile industries' effluents by using Tunisian clays as adsorbents. Zeta potential and streaming-induced potential measurements, Compt. Rendus Chem. 22 (2–3) (2019) 113–125.
- The effect of mixing speed and contact time on the process of dye adsorption using corncobs adsorbent, in: K. Pramesti, R. Kusumadewi, R. Hadisoebroto (Eds.), IOP Conference Series. Earth and Environmental Science, IOP Publishing, 2021.
- Y. Miyah, A. Lahrichi, M. Idriissi, Removal of cationic dye—Methylene blue—from aqueous solution by adsorption onto corn cob powder calcined, J. Mater. Environ. Sci. 7 (1) (2016) 96–104.
- A. Abd-Elhamid, M. Emran, M. El-Sadek, A.A. El-Shanshory, H.M. Soliman, M. Akl, et al., Enhanced removal of cationic dye by eco-friendly activated biochar derived from rice straw, Appl. Water Sci. 10 (1) (2020) 1–11.
- J. Jiang, Q. Zhang, X. Zhan, F.J.C.E.J. Chen, A multifunctional gelatin-based aerogel with superior pollutants adsorption, oil/water separation and photocatalytic properties, Chem. Eng. J. 358 (2019) 1539–1551.
- G.K. Gupta, M. Ram, R. Bala, M. Kapur, M.K.J.E.P. Mondal, S. Energy, Pyrolysis of chemically treated corncob for biochar production and its application in Cr (VI) removal, Environ. Prog. Sustain. Energy 37 (5) (2018) 1606–1617.
- Y. Yun, H. Wu, J. Gao, W. Dai, L. Deng, O. Lv, et al., Facile synthesis of Ca<sup>2+</sup>-crosslinked sodium alginate/graphene oxide hybrids as electro- and pH-responsive drug carrier, Mater. Sci. Eng. 108 (2020), 110380.
- J.S. da Silva, M.P. da Rosa, P.H. Beck, E.C. Peres, G.L. Dotto, F. Kessler, et al., Preparation of an alternative adsorbent from *Acacia Mearnsii* wastes through acetosolv method and its application for dye removal, J. Clean. Prod. 180 (2018) 386–394.
- Y. Zhao, J. Ren, T. Tan, M.-R. Babaa, Z. Bakenov, N. Liu, et al., Biomass waste inspired highly porous carbon for high performance lithium/sulfur batteries, Nanomaterials 7 (9) (2017) 260.
- R. Sharma, H. Saini, D.R. Paul, S. Chaudhary, S.P.J.E.S. Nehra, P. Research, Removal of organic dyes from wastewater using *Eichhornia crassipes*: a potential phytoremediation option, Environ. Sci. Pollut. Control Ser. (2020) 1–7.
- J.M. Jabbar, Y.A. Odusote, K.A. Alabi, I.B. Ahmed, Kinetics and mechanisms of Congo-red dye removal from aqueous solution using activated *Moringa oleifera* seed coat as adsorbent, Appl. Water Sci. 10 (6) (2020) 1–11.
- D.A. Reddy, S. Lee, J. Choi, S. Park, R. Ma, H. Yang, et al., Green synthesis of AgI-reduced graphene oxide nanocomposites: toward enhanced visible-light photocatalytic activity for organic dye removal, Appl. Surf. Sci. 341 (2015) 175–184.
- R. Leyva-Ramos, L. Bernal-Jacome, I.J.S. Acosta-Rodriguez, P. Technology, Adsorption of cadmium (II) from aqueous solution on natural and oxidized corncob, Separ. Purif. Technol. 45 (1) (2005) 41–49.
- N.K. Berber-Villamar, A.R. Netzahuatl-Muñoz, L. Morales-Barrera, G.M. Chávez-Camarillo, C.M. Flores-Ortiz, Cristiani-Urbina EJPo, Corncob as an effective, eco-friendly, and economic biosorbent for removing the azo dye Direct Yellow 27 from aqueous solutions, PLoS One 13 (4) (2018), e0196428.
- S.V. Mohan, N.C. Rao, Karthikeyan JJJohm, Adsorptive removal of direct azo dye from aqueous phase onto coal based sorbents: a kinetic and mechanistic study, J. Hazard Mater. 90 (2) (2002) 189–204.
- O.S. Bello, S.J.T. Banjo, E. Chemistry, Equilibrium, kinetic, and quantum chemical studies on the adsorption of Congo red using *Imperata cylindrica* leaf powder activated carbon, Toxicol. Environ. Chem. 94 (6) (2012) 1114–1124.
- S. Liu, Y. Ding, P. Li, K. Diao, X. Tan, F. Lei, et al., Adsorption of the anionic dye Congo red from aqueous solution onto natural zeolites modified with N, N-dimethyl dehydrobiethylamine oxide, Chem. Eng. J. 248 (2014) 135–144.
- J. Feng, H. Ding, G. Yang, R. Wang, S. Li, J. Liao, et al., Preparation of black-pearl reduced graphene oxide–sodium alginate hydrogel microspheres for adsorbing organic pollutants, J. Colloid Interface Sci. 508 (2017) 387–395.
- K.G. Bhattacharyya, A. Sharma, Azadirachta indica leaf powder as an effective biosorbent for dyes: a case study with aqueous Congo Red solutions, J. Environ. Manag. 71 (3) (2004) 217–229.
- X. Rong, F. Qiu, J. Qin, H. Zhao, J. Yan, DJJoi Yang, et al., A facile hydrothermal synthesis, adsorption kinetics and isotherms to Congo Red azo-dye from aqueous solution of NiO/graphene nanosheets adsorbent, J. Ind. Eng. Chem. 26 (2015) 354–363.
- K.V. Kumar, V. Ramamurthi, Sivanesan SJJoc, i science, Modeling the mechanism involved during the sorption of methylene blue onto fly ash, J. Colloid Interface Sci. 284 (1) (2005) 14–21.

- [47] A. Riegas-Villalobos, F. Martínez-Morales, R. Tinoco-Valencia, L. Serrano-Carreón, B. Bertrand, M.R.J.B. Trejo-Hernández, Efficient removal of azo-dye Orange II by fungal biomass absorption and laccase enzymatic treatment, *Biotech* 10 (4) (2020) 1–10.
- [48] O. Yesilada, D. Asma, S.J.P.B. Cing, Decolorization of textile dyes by fungal pellets, *Process Biochemistry* 38 (6) (2003) 933–938.
- [49] M. Hashim, A. Ahmed, S.A. Ali, S.E. Shirsath, M.M. Ismail, R. Kumar, et al., Structural, optical, elastic and magnetic properties of Ce and Dy doped cobalt ferrites, *J. Alloys Compd.* 834 (2020), 155089.
- [50] L. Ding, B. Zou, W. Gao, Q. Liu, Z. Wang, Y. Guo, et al., Adsorption of Rhodamine-B from aqueous solution using treated rice husk-based activated carbon, *Colloids Surf. A Physicochem. Eng. Asp.* 446 (2014) 1–7.
- [51] J. Ma, Z. Jiang, J. Cao, F.J.C. Yu, Enhanced adsorption for the removal of antibiotics by carbon nanotubes/graphene oxide/sodium alginate triple-network nanocomposite hydrogels in aqueous solutions, *Chemosphere* 242 (2020), 125188.
- [52] R. Santos, É.F. Silva, E.J. Dantas, E.D. Oliveira, T.B. Simões, Í.R. Araújo, et al., Potential reuse of PET waste bottles as a green substrate/adsorbent for reactive black 5 dye removal, *Water, Air, Soil Pollut.* 231 (11) (2020) 1–16.
- [53] C. Jiao, T. Li, J. Wang, H. Wang, X. Zhang, X. Han, et al., Efficient removal of dyes from aqueous solution by a porous sodium alginate/gelatin/graphene oxide triple-network composite aerogel, *J. Polym. Environ.* 28 (2020) 1492–1502.
- [54] A. Oussalah, Boukerroui A.JE-MJfEI, Removal of cationic dye using alginate–organobentonite composite beads, *J. Environ. Int.* 5 (3) (2020) 1–10.
- [55] A. Pettignano, N. Tanchoux, T. Cacciaguerra, T. Vincent, L. Bernardi, E. Guibal, et al., Sodium and acidic alginate foams with hierarchical porosity: preparation, characterization and efficiency as a dye adsorbent, *Carbohydr. Polym.* 178 (2017) 78–85.
- [56] M.A. Ahmad, N.A.B. Ahmed, K.A. Adegoke, O.S. Bello, Sorption studies of methyl red dye removal using lemon grass (*Cymbopogon citratus*), *Chemical Data Collections* 22 (2019), 100249.
- [57] D.J.G. Rondina, D.V. Ymbong, M.J.M. Cadutdut, J.R.S. Nalasa, J.B. Paradero, V.I.F. Mabayo, et al., Utilization of a novel activated carbon adsorbent from press mud of sugarcane industry for the optimized removal of methyl orange dye in aqueous solution, *Appl. Water Sci.* 9 (8) (2019) 1–12.
- [58] E.R. Haqiqi, D.I. Hikmawati, Influence of chicken EggShell powder ratio with coarse rice husk on methyl orange removal from aqueous solution, *CHEESA: Chemical Engineering Research Articles* 2 (1) (2019) 33–41.
- [59] C.K. Enebeaku, N.J. Okorochoa, E.E. Uchechi, I.C. Ukaga, Adsorption and equilibrium studies on the removal of methyl red from aqueous solution using white potato peel powder, *Int. Lett. Chem. Phys. Astron.* 72 (2017) 52.
- [60] Synthesis of mesopore silica composite from rice husk with activated carbon from coconut shell as absorbent methyl orange color adsorbent, in: Y. Yusmaniar, E. Erdawati, Y. Ghifari, D. Ubit (Eds.), *IOP Conference Series: Materials Science and Engineering*, IOP Publishing, 2020.
- [61] G. Ghosh, T. Chakraborty, S. Zaman, M. Nahar, A. Kabir, Removal of methyl orange dye from aqueous solution by a low-cost activated carbon prepared from Mahagoni (*Swietenia mahagoni*) bark, *Pollution* 6 (1) (2020) 171–184.
- [62] H. Park, J. Kim, Y.-G. Lee, K. Chon, Enhanced adsorptive removal of dyes using Mandarin peel biochars via chemical activation with  $\text{NH}_4\text{Cl}$  and  $\text{ZnCl}_2$ , *Water* 13 (11) (2021) 1495.
- [63] U. Das, I. Sharmin, N. Islam, Removal of Cr (VI) Ion and Methyl Red from Wastewater Using Agricultural Waste Bioadsorbents, 2017.